Dynamics in Physisorbed Monolayers of 5-Alkoxy-isophthalic Acid Derivatives at the Liquid/Solid Interface Investigated by Scanning Tunneling Microscopy

André Gesquière,[a] Mohamed M. Abdel-Mottaleb,[a] Steven De Feyter,*[a] Frans C. De Schryver,*[a] Michel Sieffert,[b] Klaus Müllen,[b] Anna Calderone,[c] Roberto Lazzaroni,[c] and Jean-Luc Brédas[c]

Abstract: Monolayers of isophthalic acid derivatives at the liquid/solid interface have been studied with scanning tunneling microscopy (STM). We have investigated the dynamics related to the phenomenon of solvent co-deposition, which was previously observed by our research group when using octan-1-ol or undecan-1-ol as solvents for 5-alkoxy-isophthalic acid derivatives. This solvent co-deposition has now been visualized in real-time (two frames per second) for the first time. Dynamics of individual molecules were investigated in mixtures of semi-fluorinated molecules with video-STM. The specific contrast arising from fluorine atoms in STM images allows us to use this functionality as a probe to analyze the data obtained for the mixtures under investigation. Upon imaging the same region of a monolayer for a period of time we observed that non-fluorinated molecules progressively substitute the fluorinated molecules. These findings illustrate the metastable equilibrium that exists at the liquid/solid interface, between the physisorbed molecules and the supernatant solution.

Keywords: liquid/solid interface · monolayers · scanning probe microscopy · self-assembly

Introduction

With scanning tunneling microscopy (STM) organic monolayers can be studied with submolecular resolution at the liquid/solid interface. This type of monolayers, which are formed by spontaneous self-organization of molecules from solution on solid substrates, has been studied for a wide variety of compounds.[1] Besides functionality, chirality and photoreactivity have also been investigated at the liquid/solid interface.[2],[3]

[a] Dr. S. De Feyter, Prof. Dr. F. C. De Schryver, Drs. A. Gesquière, Drs. M. M. Abdel-Mottaleb
University of Leuven (KULeuven), Department of Chemistry
Laboratory of Molecular Dynamics and Spectroscopy
Celestijnenlaan 200-F, 3001 Heverlee (Belgium)
E-mail: steven.defeyter@chem.kuleuven.ac.be
frans.deschryver@chem.kuleuven.ac.be

[b] Drs. M. Sieffert, Prof. Dr. K. Müllen
Max-Planck Institute for Polymer Research
Ackermannweg 10, 55128 Mainz (Germany)

[c] Dr. A. Calderone, Dr. R. Lazzaroni, Prof. Dr. J.-L. Brédas
Service de Chimie des Matériaux Nouveaux
Centre de Recherche en Electronique et Photonique Moléculaires
Université de Mons-Hainaut,
Place du Parc, 20, 7000 Mons (Belgium)

STM does not only allow the visualization of the ordering within monolayers, but also the study of the dynamics within these monolayers. The range of dynamic phenomena that can be investigated by STM is limited by the nature of the STM experiment, which is generally slow compared with the timescale of single molecule dynamics.

Several spontaneous dynamic phenomena have been visualized both in pure and mixed monolayer systems at the liquid/solid interface. Stabel et al. investigated the two-dimensional structure of 2-hexadecyl-anthraquinone monolayers.[4] The analysis suggests a rather loose packing with nonoptimized intermolecular interactions. The authors propose that the STM-images present the average structure between two oscillating densely packed monolayer structures.

Ostwald ripening describes the growth of larger particles at the expense of smaller particles. The thermodynamic driving force in two dimensions is the reduction of the circumference-to-area ratio and thereby the lowering of the interfacial or line energy. Stabel et al. studied this phenomenon in two-dimensional systems with STM.[5] They observed that small domains in 2-hexadecyl-anthraquinone and tetradodecyl-octathiophene monolayers shrink and finally disappear. Reorientation of molecules and lamellar fragments with respect to the graphite substrate has been invoked to explain the observed Ostwald ripening.

 © WILEY-VCH Verlag GmbH, D-69451 Weinheim, 2000 0947-6539/00/0620-3739 $ 17.50+.50/0

A variable temperature fast STM was used to observe the order-disorder transition in monolayers of alkanes at the liquid/graphite interface.[6] At the interface between a neat melt of a long-chain alkane and a solution of this long-chain alkane disordered lamellae and a columnar phase are found.

Dynamic processes have also been reported for mixed monolayers of triacontane/triacontanol by Venkataraman et al.[7] They observed that triacontane and triacontanol form separate domains on the graphite substrate. The alcohol molecules are found to adsorb preferentially on the substrate and they have a tendency to displace the alkane molecules off the surface. This molecular motion in adlayers of the mixtures is the main reason for the noisier images that were obtained for the mixtures when compared with the single-component solutions. Mixed octadecanol/tetracosanol monolayers physisorbed on highly oriented pyrolytic graphite (HOPG) were imaged by Elbel et al.[8] They found that the molecular organization is dependent of concentration ratio between the two components in the mixture. Dynamics could be observed for an ordered arrangement consisting of mixed double lamellae of octadecanol and tetracosanol. For this ordering molecular dynamics could be detected. The composition of the lamella was found to fluctuate, while maintaining an overall densely packed double lamella structure. This was explained by assuming a correlated desorption-readsorption process of octadecanol/tetracosanol pairs.

Molecular motion at domain boundaries in mixed monolayers of fatty acids adsorbed on graphite has recently been observed.[9] Hibino et al. observed a dynamic exchange of the two kinds of observed lamellae, which consist of myristic acid and behenic acid; this indicates an adsorption–desorption process of molecules on the graphite surface.

In this paper we report on dynamics occurring in monolayers of isophthalic acid (ISA) derivatives at the liquid/solid interface, detected by scanning tunneling microscopy. The presented images show the rearrangement of the molecules adsorbed on the surface due to reorientation and adsorption-desorption of the molecules in the monolayer.

Experimental Section

Synthesis of the compounds discussed in the paper: The synthesis of Hn-ISA (Figure 1b) was reported previously.[10]

Dimethyl 5-(-hexenyloxy)isophthalate: Dimethyl 5-hydroxyisophthalate (3.6 g, 17 mmol) and potassium carbonate (2.8 g, 20 mmol) were stirred in dry *N*,*N*-dimethylformamide (100 mL) for one hour at 80 °C. To this mixture, 6-bromohex-1-ene (2.8 g, 17 mmol) was added and the mixture was stirred for 10 h. The solvent was then evaporated and the residue mixed with water followed by extraction with dichloromethane (5 × 50 mL). The combined organic phases were dried over magnesium sulphate. The mixture was concentrated through evaporation of dichloromethane and purified by column chromatography on silica gel (ethyl acetate/petroleum ether 1:9) to obtain pure dimethyl 5-(-hexenyloxy)isophthalate as a colorless oil (4.02 g, 13.7 mmol, 81 %); ^{1}H NMR (250 MHz, $CDCl_3$, 25 °C): $\delta = 8.23$ (d, $^4J(H,H) = 1.55$ Hz, 1H, ArH), 7.71 (d, $^4J(H,H) = 1.55$ Hz, 2H, ArH), 5.88–5.72 (m, 1H, CH=CH_2), 5.05–4.93 (m, 2H, CH=CH_2), 4.02 (t, $^3J(H,H) = 6.2$ Hz, 2H, OCH_2), 3.91 (s, OCH_3, 6H), 2.15–2.06 (m, 2H, CH_2), 1.85–1.74 (m, 2H, CH_2), 1.62–1.49 (m, 2H, CH_2); ^{13}C NMR (75 MHz, $CDCl_3$, 25 °C): $\delta = 166.19$, 159.16, 138.35, 131.68, 122.27, 119.79, 114.85, 68.36, 52.37, 33.33, 28.48, 25.20; MS-FD: *m*/*z*: 292.3 $[M]^+$; elemental analysis calcd (%) for $C_{16}H_{20}O_5$: C 75.74, H 6.90; found: C 75.66, H 6.89.

Dimethyl 5-(7,7,8,8,9,9,10,10,11,11,12,12,13,13,14,14,15,15,16,16,17,17,18,18,18-pentacosafluoro-*n*-octadecyloxy)isophthalate: 1-Iodoperfluorododecane (3.0 g, 4.02 mmol) and 5-(ω-hexenyloxy)isophthalate (1.17 g, 4.0 mmol) were added into a two-necked-round bottom flask equipped with a reflux condenser, an argon inlet and a magnetic stirrer. The mixture was homogenized by heating to 80 °C. During the following 2 h AIBN (0.075 g, 0.457 mmol) was added in small portions and the reaction mixture was stirred for another 5 h. The reaction was followed by ^{1}H NMR. After cooling to room temperature, the mixture solidified to a yellow waxy solid. The crude product (4.0 mmol) was dissolved in dry toluene (10 mL) under argon. Tri-n-butyltin hydride (3.2 mL, 12.0 mmol) and AIBN (0.082 g, 0.5 mmol) were added and the solution was stirred for 12 h at 80 °C. Methanol was added to decompose the excess of hydride. After cooling to room temperature, a white precipitate was isolated by suction filtration. The product was isolated after column chromatography on silica gel (dichloromethane/petroleum ether 3:2) as a colorless solid (2.44 g, 2.67 mmol, 67 %). M.p. 97 °C; ^{1}H NMR (250 MHz, $CDCl_3$, 25 °C): $\delta =$ 8.02 (s, 1H, ArH), 7.71 (s, 2H, ArH), 4.05 (t, $^3J(H,H) = 6.3$ Hz, 2H, OCH_2), 3.91 (s, 6H, OCH_3), 2.16–1.95 (m, 2H, CH_2CF_2), 1.86–1.76 (m, 2H, OCH_2CH_2), 1.69–1.40 (m, 2H, CH_2); ^{13}C NMR (75 MHz, $CDCl_3$, 25 °C):$\delta = 166.18$, 159.11, 131.74, 122.86, 119.78, 68.27, 52.37, 30.81, 28.84, 27.01, 25.70, 20.08; MS-FD: *m*/*z*: 912.4 $[M]^+$; elemental analysis calcd (%) for $C_{28}H_{21}F_{25}O_5$: C 36.86, H 1.94; found: C 36.78, H 1.92.

Dimethyl 5-(7,7,8,8,9,9,10,10,11,11,12,12,13,13,14, 14,15,15,16,16,17,17,18,18,18-pentacosafluoro-*n*-octodecyloxy)isophthalic acid ($F_{12}H_6$-ISA): The hydrolysis of dimethyl 5-((ω-perfluorododecyl)hexyloxy)isophthalate (2.0 g, 2.2 mmol) was performed in a solution of sodium hydroxide (0.168. g, 3.0 mmol) in ethanol/water 2:1, which was stirred for 6 h under reflux. The solution was cooled to room temperature. The white precipitate obtained after addition of conc. HCl was filtered, washed with water, and dried under high vacuum. The crude acid was recrystallized from ethyl acetate to yield a pure colorless and crystalline product (1.84 g, 2.08 mmol, 95 %); M.p. 197 °C; ^{1}H NMR (250 MHz, DMSO, 55 °C): $\delta = 8.02$ (s, 1H, ArH), 7.56 (s, 2H, ArH), 3.96 (t, $^3J(H,H) = 6.0$ Hz, 2H), 2.08–1.90 (m, 2H, CH_2, CF_2); 1.70–1.62 (m, 2H, OCH_2CH_2), 1.47–1.36 (m, 6H, CH_2); ^{13}C NMR (75 MHz, DMSO, 55 °C): $\delta = 165.93$, 158.44, 132.41, 121.89, 118.66, 67.70, 29.65, 27.91, 27.65, 24.56, 19.14; MS-FD: *m*/*z*: 884.3 $[M]^+$; elemental analysis calcd (%) for $C_{26}H_{17}F_{25}O_5$: C 35.31, H 1.94; found: C 35.23, H 2.02.

Scanning tunneling microscopy: Prior to imaging, all compounds under investigation were dissolved in octan-1-ol or undecan-1-ol (Aldrich, 99 %) and a drop of this solution was applied on a freshly cleaved surface of highly oriented pyrolytic graphite. The STM images were acquired in the variable current mode (constant height) under ambient conditions. In the STM images, white corresponds to the highest and black to the lowest measured tunneling current. STM experiments were performed using a Discoverer scanning tunneling microscope (Topometrix Inc., Santa Barbara, CA) along with an external pulse/function generator (Hewlett Packard 8111 A), with negative sample bias. Tips were electrochemically etched from Pt/Ir wire (80 %:20 %, diameter 0.2 mm) in a 2 N KOH/6 N NaCN solution in water. The scanning speed of the Topometrix Discoverer STM in standard mode is limited to seven seconds per image consisting of 200 lines and 200 pixels per line. After modification, the scanning speed improved to two images per second (video-STM). Most home-built systems described in literature can acquire several frames per second, although imaging rates up to 20 frames per second have been reported.[1a,11] However, when frame rates of ten frames per second or even higher are reported, one should keep in mind that in these cases, the presented "snapshots" are in fact several averaged frames. This is done in order to reduce the considerable amount of noise that is inherent to the high scanning speed.

The feedback of the video-STM system is controlled by the Topometrix hardware, the scanning and image acquisition is regulated by a home built setup. Four HP 33120A function generators, set up as a phase-lock assembly, control the scanning of the Stm tip as well as the storage of the STM image in the image buffer of an Arlunya TF6000 image processor. In this way, the tunneling current at each *x*,*y*-coordinate is mapped to the correct pixel. The STM images are recorded in real-time (two frames per second) on videotape. Individual images can be retrieved by PC.

The experiments were repeated in several sessions using different tips to check for reproducibility and to avoid artifacts. Different settings for the

© WILEY-VCH Verlag GmbH, D-69451 Weinheim, 2000
0947-6539/00/0620-3740 $ 17.50+.50/0 *Chem. Eur. J.* **2000**, *6*, No. 20

tunneling current and the bias voltage were used, ranging from 0.3 nA to 1.3 nA and −10 mV to −1.5 V, respectively. During imaging, we detected little drift of the STM system and care was taken that the same region of the monolayer was imaged during consecutive scans. All STM images contain raw data and are not subjected to any manipulation or image processing. The presented snapshots are single frames.

Molecular mechanics calculations: The molecular mechanics calculations have been performed on periodic systems with the Cerius[2] package developed by Molecular Simulations Inc. The potential energy is described with the Universal Force Field (UFF), with partial atomic charges set to zero.[12],[13] The long-range non-bonding interactions are calculated by using the Ewald method (the parameters being estimated within the program). The considered plane of graphite is composed of 20×30 fused rings and contains 1200 carbon atoms. The atomic positions are fixed during the energy minimization processes. We emphasize that we have tested this approach on small systems consisting of one CH_4 or one CF_4 molecule adsorbed on graphite. The corresponding results are in agreement with previous experimental and theoretical data obtained with post Hartree–Fock quantum chemical calculations.[18b]

Results and Discussion

Dynamic processes occurring at the liquid/solid interface, between monolayers adsorbed on the substrate and the supernatant solution, are illustrated by the systems investigated within our research group. Specifically, we report the visualization of the exchange of molecules between monolayers of isophthalic acid derivatives adsorbed on HOPG and the supernatant solution. The molecular structures of the compounds under investigation are shown in Figure 1.

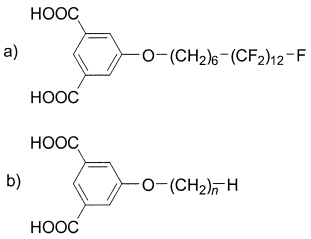

Figure 1. Chemical structure of the compounds under investigation: (a) 5-((ω-perfluorododecyl)hexyloxy)isophthalic acid ($F_{12}H_6$-ISA); (b) 5-(ω-alkoxy)isophthalic acid (Hn-ISA, $n = 18, 20$).

Insertion of solvent molecules in H_{20}-ISA monolayers: Upon applying a drop of a solution of H_{20}-ISA in octan-1-ol onto a freshly cleaved graphite surface highly ordered monolayers, spontaneously formed by physisorption, can be observed with STM. Figure 2a shows an STM image of the structure of such a monolayer. The aromatic moiety of the H_{20}-ISA molecules is visible as a bright spot.[14] The wide darker bands correspond to the location of the alkoxy-chains, which are fully interdigitated, while the narrow ones with a similar contrast reflect the location of octan-1-ol molecules co-deposited between adjacent H_{20}-ISA lamellae.[15] The short solvent molecules can be observed on the substrate since the carboxyl groups of the ISA head groups form hydrogen bonds with the hydroxyl group of the solvent molecules. Co-deposition, in this case the adsorption of solvent molecules from the supernatant solution in the monolayer structure, is a dynamic process. This is illustrated in Figure 2. At the left-hand side of each picture one can see how solvent molecules are progressively incorporated between adjacent H_{20}-ISA lamellae. The newly formed solvent lamella interleaves the two adjacent H_{20}-ISA lamellae. A domain boundary at the left-hand bottom corner is used as a reference point. The co-deposition process was completed within two minutes. Not surprisingly, this process is initiated at a domain boundary, typically a region with free volume and hence increased dynamics. In contrast to Ostwald ripening, which only involves the reorientation of molecules and lamellar fragments within the monolayer, co-deposition involves both exchange with the supernatant solution as well as reorientation of the lamellar fragments. For instance, Figure 2 shows that co-adsorption of octan-1-ol molecules induces a cooper-

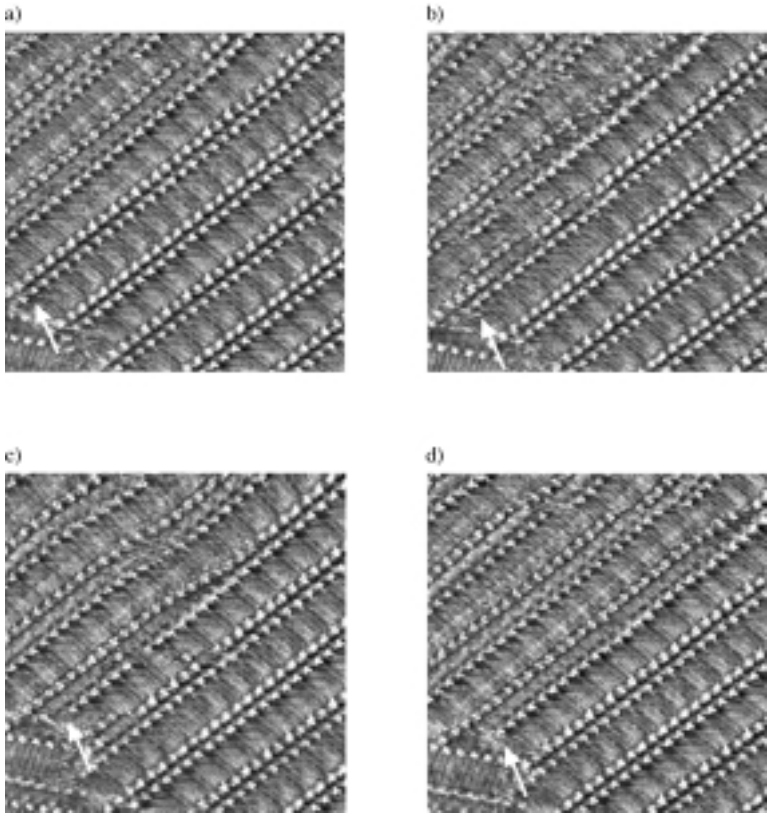

Figure 2. A series of STM pictures of the same area of a H_{20}-ISA monolayer deposited from octan-1-ol obtained at a) $t = 0$ s, b) $t = 32$ s, c) $t = 89$ s, and d) $t = 120$ s. The arrow indicates where the insertion of solvent molecules between two adjacent lamellae is initiated. The wide lamellae consist of H_{20}-ISA molecules. The narrow lamellae are built up by solvent molecules. Image sizes are 23.0×23.0 nm^2. $I_{set} = 1.0$ nA, $V_{bias} = -0.8$ V.

ative shift of the lamellae to the upper-left of the image. This is expressed in the image by the appearance of a wavelike pattern. The lamellae in the lower right of the image are basically unaffected by the insertion process.

A detailed quantitative analysis of this particular co-deposition process reveals a linear relationship between the number of octan-1-ol molecules that adsorb inbetween the H_{20}-ISA lamellae and the timescale of the process. It was therefore possible to obtain the insertion rate that characterizes the observed process, which was found to be 0.4 molecules per second. Notably this rate is only applicable to this particular example. In general, we did not find this kind of linear relationship. For example, in the two systems described hereafter in this section the number of solvent molecules that build-up the solvent lamellae under consideration was found to fluctuate.

These data were obtained with a commercial STM system capable of collecting one STM image every seven seconds. We took this study a step further by investigating dynamic phenomena related to solvent co-deposition by means of a video-STM, which enables us to acquire data in a continuous mode (two frames per second).

Figure 3a shows an STM image of the structure of a monolayer of H_{20}-ISA dissolved in undecan-1-ol. The solid arrow indicates a region where solvent molecules are incorporated in the H_{20}-ISA monolayer. The dashed arrow indicates a boundary between two H_{20}-ISA lamellae, one with (left) and one without (right) solvent molecules co-deposited adjacent to it. The four ISA groups directly above these solvent molecules are used as a reference to keep track of the progress of the dynamic process (encircled in Figure 3a). With video-STM, we were able to observe dynamic changes occurring at the location indicated by the dashed arrow. Starting from this location, solvent molecules are progressively inserted in between the H_{20}-ISA lamellae. In Figure 3b, which is a snapshot taken from a video tape forty-one seconds after Figure 3a, the solvent lamella has advanced towards the domain boundary in the top right section of the image (indicated by the solid line). At the same time, the isophthalic acid reference row has expanded along the growth direction of the solvent lamella: now eight ISA groups interacting with these solvent molecules can be distinguished. This local change of the monolayer structure also has an impact on the neighboring lamella. Simultaneously with the insertion of the solvent molecules, other undecan-1-ol molecules desorb from the surface (solid arrow). Due to the extra space taken up by the new co-adsorbed solvent molecules, the adjacent H_{20}-ISA lamella shifts towards the top of the image, and thereby forces other undecan-1-ol molecules out of the monolayer. Naturally, the distance over which the H_{20}-ISA lamella is shifted corresponds to the width of a undecan-1-ol lamella. The molecular motions during this rearrangement were faster than the speed of image acquisition. Solvent molecules adsorbed or desorbed between scans, thus the adsorption and desorption process takes less than 0.5 s (the time required to obtain one image). Based on the time required to obtain one image and the number of scan lines that build-up this image a rough estimate of the exchange rate between the monolayer and the solution on top can be made. An ISA group is seven scan lines in the presented images. The time required to scan one line is 2.4 ms. This means that the H_{20}-ISA molecules have a residence time on the surface of at least 16.8 ms. The undecan-1-ol molecules also appear stable over several scan lines. Consecutive images usually show the same general organization. This implies that the overall structure of the monolayer in the observed region remains stable for at least 0.5 s. Twenty-six seconds after the frame in Figure 3b was obtained, the solvent lamella has progressed all the way to the domain boundary, as shown in Figure 3c. The actual residence time of individual molecules can not reliably be determined. Although the overall structure appears to remain unchanged, molecules are most probably exchanging between consecutive images, even though it is not possible to observe this. This makes a more detailed quantitative discussion precarious. Therefore we moved to the study of semi-fluorinated molecules. The specific contrast of the fluorinated chain in the STM images serves as a label to follow the molecular exchanges as a function of time. This will be discussed further in the text.

On a few occasions, a double row of undecan-1-ol molecules was observed. The width of such a double row is 3.1 nm, which is somewhat smaller than the width of an H_{20}-ISA lamella (3.7 nm). This explains why a double row of undecan-1-ol molecules can adsorb in an H_{20}-ISA adlayer

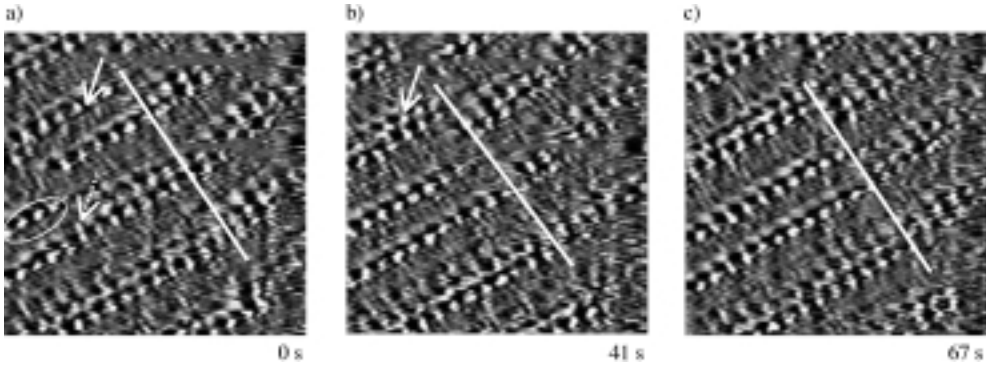

Figure 3. Snapshots taken from videotape, showing STM images of an H_{20}-ISA monolayer formed by physisorption from a solution in undecan-1-ol on HOPG. The time of the first image is arbitrarily set to zero. a) Solvent molecules incorporate in between H_{20}-ISA lamellae during imaging. The dashed arrow indicates where the insertion process is taking place. The encircled area indicates the four isophthalic groups that serve as a reference to follow the observed molecular motions. The solid arrow indicates where solvent molecules are consequently expelled from the monolayer (shown in b). c) The solvent lamella extends all the way to the domain boundary (solid line). Image sizes are 15.0×15.0 nm^2. $I_{set} = 0.9$ nA, $V_{bias} = -0.6$ V.

© WILEY-VCH Verlag GmbH, D-69451 Weinheim, 2000
0947-6539/00/0620-3742 $ 17.50+.50/0 *Chem. Eur. J.* **2000**, *6*, No. 20

without major disturbance of the monolayer structure. In Figure 4a two adjacent solvent lamellae are visible in the center of the image. Figure 4b and Figure 4c show how the double solvent lamella breaks up. At this stage H_{20}-ISA molecules adsorb at the same location as the solvent molecules, thereby replacing them. However, simultaneously another double row of solvent molecules appears immediately above the expanding H_{20}-ISA lamella. At this time, we are not able to determine if the solvent molecules stay adsorbed on the surface and slide upwards over a distance corresponding to the width of a H_{20}-ISA lamella (thereby expelling the neighboring H_{20}-ISA molecules from the monolayer) or if the two adjacent solvent lamellae and the neighboring H_{20}-ISA lamella desorb cooperatively and are replaced by molecules from the solution on top of the monolayer. When the dynamic process is completed, it appears as if the double lamella of solvent molecules and the H_{20}-ISA lamella directly above have traded places, as shown in Figure 4d. The tip was then translated during scanning in such a way that the rows of solvent molecules again appear in the middle of the image (Figure 4e). The images in Figure 4f–h show that this less-favorable packing is ultimately replaced by the more stable arrangement of lamellae of the isophthalic acid derivative interspersed by a single row of solvent molecules. Previous reports from our research group, mentioned in the introduction, demonstrate that the latter arrangement is indeed the most favorable for the systems considered in this paper.[15] From these observations we find that double lamellae of undecan-1-ol are stable within an H_{20}-ISA monolayer on a timescale of minutes. The time that the molecules remain on the graphite surface was determined using the principle explained above and was in this case at least 15 ms. The blurry area in Figure 4f could be observed during two seconds. In this time interval the double undecan-1-ol lamella and an H_{20}-ISA lamella (58 molecules) desorbed from the surface and the structure as seen in Figure 4g was formed. The entire process came about in 73 seconds.

Exchange of fluorinated and non-fluorinated isophthalic acid derivatives in their mixed monolayers: The experiments in the previous section clearly illustrate the dynamics and structural changes that take place within monolayers at the liquid/solid interface. However, these experiments do not provide information about the exchange or mobility of individual molecules in domains that do not undergo major structural changes. In view of that we introduced semi-fluorinated isophthalic acid derivatives, which can act as markers that allow us to study this type of dynamics.

In a previous paper we reported on the two-dimensional organization of semi-fluorinated isophthalic acid derivatives physisorbed on the basal plane of HOPG.[16] Upon mixing of a fluorinated isophthalic acid derivative with its non-fluorinated analogues, mixed monolayers are formed. No separate domains of non-fluorinated and semi-fluorinated molecules could be observed. Individual lamellae are composed of a random mixture of fluorinated and non-fluorinated molecules. Now, this imaging process has been taken a step further by studying dynamics in these mixed monolayers. Specifically, monolayers physisorbed from a mixture of $F_{12}H_6$-ISA with

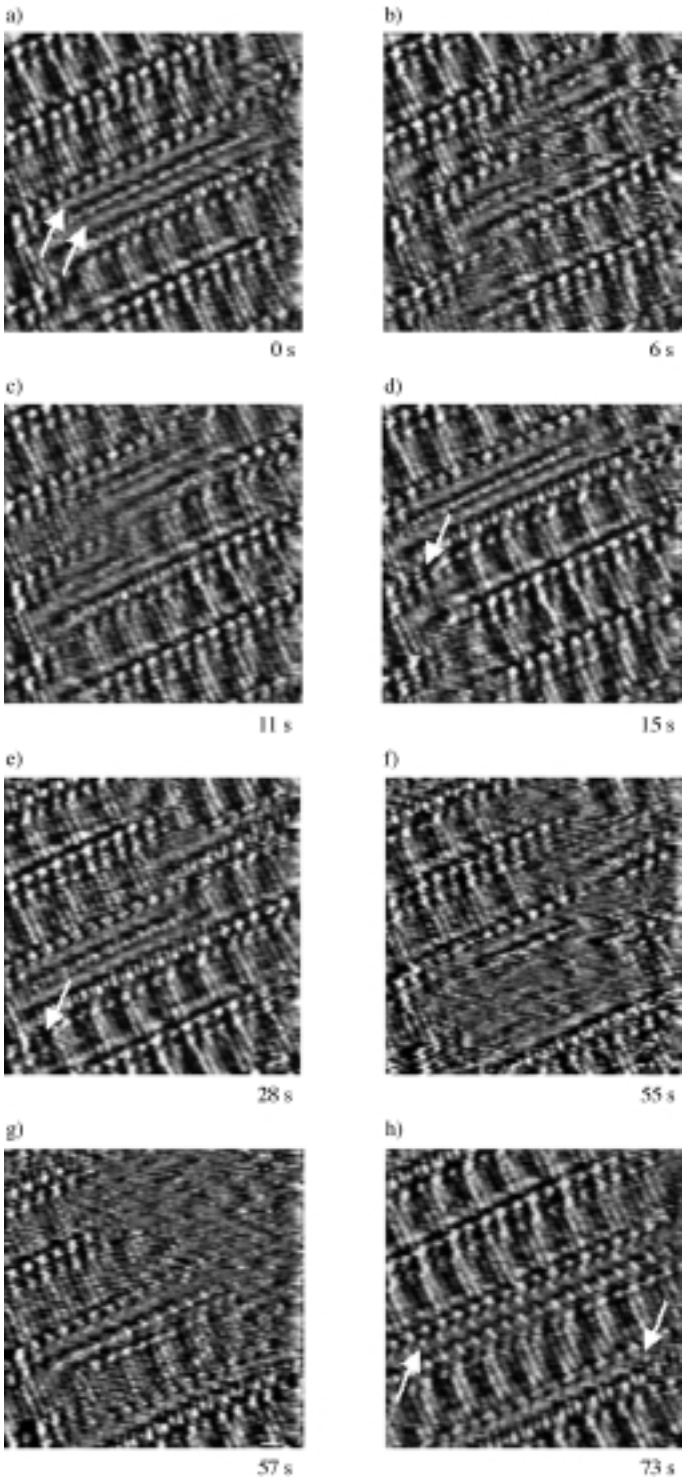

Figure 4. Snapshots taken from a video-STM movie. The time of the first image is arbitrarily set to zero. a) A double row of undecan-1-ol molecules can be recognized in the center of image (indicated by arrows). This structure breaks up and re-emerges in the top of the image b) and c). d)–e) After the completion of this restructuring the scanning area (identical size) was centered again around the double lamella. For clarity, an arrow points to a reference point. f) At the end the double lamella disintegrates. Because of the mobility of the molecules during the reorganization this area appears distorted in the image. g) A more stable arrangement composed of lamellae of the isophthalic acid derivative interspersed by a single row of solvent molecules appears (indicated by arrows in h). The domain visible in the top right of image e) and f) disappears and is replaced by the expanding restructured domain, as can be seen in image h). Image sizes are 16.5×16.5 nm^2. $I_{set} = 0.9$ nA, $V_{bias} = -0.85$ V.

H_{18}-ISA (concentration ratio 1:1) in octan-1-ol have been studied. When the same area of such a monolayer was imaged during an extended period of time a dynamic process occurring at the graphite surface could be observed, as shown in the image series in Figure 5a – f. Both semi-fluorinated and non-fluorinated molecules can be distinguished by their characteristic STM contrast. The perfluorinated part of the alkyl chain appears as a black band, due to a relative decrease in tunneling current compared with the non-fluorinated alkyl chains. Hence, this functionality is a good marker that allows us to study the exchange of molecules between the liquid phase and the physisorbed monolayer quantitatively. The observed contrast for the perfluorinated part of the alkyl chain is in agreement with a previous study of a single fluorine atom substituted stearic acid physisorbed on graphite, and supported by theoretical calculations.[17, 18] The bright spots correspond to the location of the isophthalic acid groups. The non-fluorinated part of the alkyl chain can be seen as a darker band with respect to the isophthalic acid groups. The $F_{12}H_6$-ISA molecules were found to be distributed sparsely over the monolayer.

At first, two semi-fluorinated molecules are visible in the STM image, shown in Figure 5a. These molecules are indicated by the arrows. The bright edges around the black bands of the semi-fluorinated molecules are scanning artifacts. These were always observed in the vicinity of a fluorinated alkyl chain during the course of our experiments. In Figure 5b, an additional fluorinated molecule has adsorbed on the surface, as can be seen in the top left of the imaged area. In Figure 5c, this semi-fluorinated molecule has desorbed, while the two initially imaged semi-fluorinated molecules remain on the graphite surface. The residence time of this third molecule on the surface was 8.0 s. While scanning from the top of the image shown in Figure 5d to the bottom only a part of the semi-fluorinated chain of the $F_{12}H_6$-ISA molecule left in the image could be visualized, as can be seen in the encircled area. The hind part of the fluorinated alkyl chain is no longer visible. This is explained by the fact that during the acquisition of a scanline over the $F_{12}H_6$-ISA molecule, this molecule was exchanged for an H_{18}-ISA molecule. Thus the exchange rate is faster than the time needed to obtain one scanline, in this case 4.3 ms. In the subsequent scan taken immediately after Figure 5d it is clear that the $F_{12}H_6$-ISA molecule has indeed been substituted by a non-fluorinated H_{18}-ISA molecule.

In Figure 5f the remaining fluorinated molecule has also desorbed from the graphite surface and has been replaced by a non-fluorinated molecule. The entire process came about in 58 s.

In general, the residence time of a fluorinated molecule was found to vary from several seconds to several minutes. In some cases we even found the residence time to be tens of minutes. These residence times are much higher than those observed by Stevens et al. for mixtures of long-chain alcohols and long-chain thiols.[19] This demonstrates the impact of the hydrogen bonding between neighboring isophthalic acid groups and between the isophthalic acid groups and the solvent molecules in the monolayer. Because of this type of hydrogen bonding highly stabilized two-dimensional crystals are formed for which the exchange rate of molecules between the monolayer and the solution is considerably reduced.

In order to reveal the relative importance of adsorbate-substrate and adsorbate – adsorbate interactions that lead to

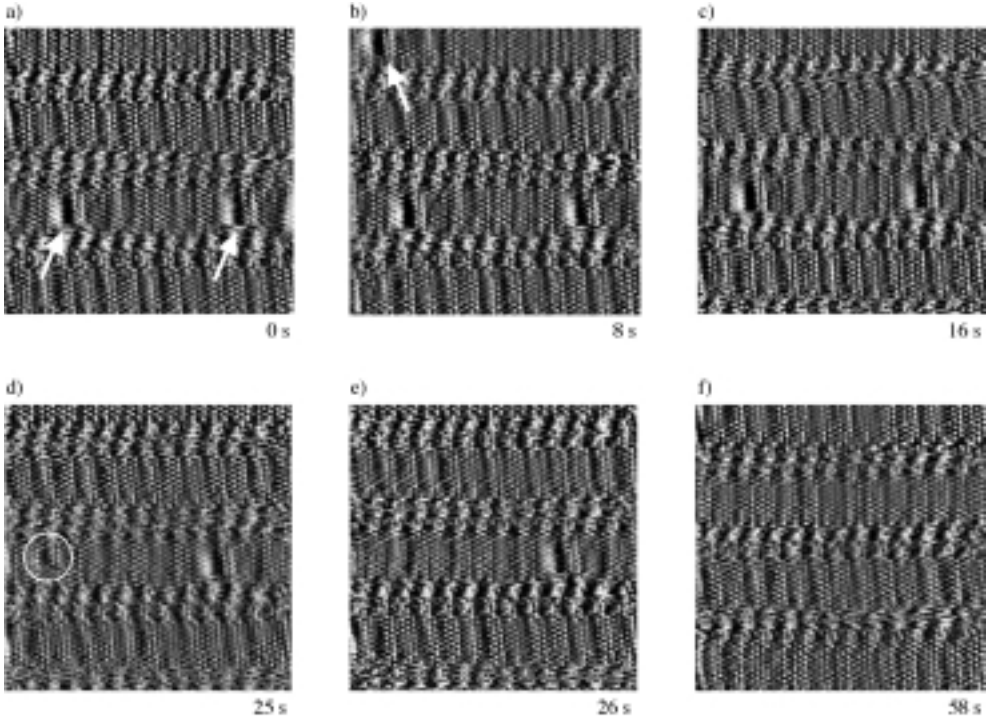

Figure 5. Snapshots taken from an STM videotape. The time of the first image is arbitrarily set to zero. a) Two $F_{12}H_6$-ISA molecules are initially co-adsorbed in an H_{18}-ISA monolayer. The arrows indicate the two $F_{12}H_6$-ISA molecules. b) A third $F_{12}H_6$-ISA molecule has adsorbed in an H_{18}-ISA lamella (indicated by arrow). c) Eight seconds later this molecule is exchanged for an H_{18}-ISA molecule. d) The encircled area indicates the partly imaged semi-fluorinated alkyl chain. The $F_{12}H_6$-ISA molecule desorbs while the tip is scanning over it. e) The remaining $F_{12}H_6$-ISA molecule is replaced by an H_{18}-ISA molecule as well, as can be seen in f). Image sizes are 12.5×12.5 nm^2. $I_{set} = 1.1$ nA, $V_{bias} = -0.38$ V.

© WILEY-VCH Verlag GmbH, D-69451 Weinheim, 2000
0947-6539/00/0620-3744 $ 17.50+.50/0 *Chem. Eur. J.* **2000**, *6*, No. 20

the gradual desorption of the fluorinated molecules and their replacement by non-fluorinated ones, molecular mechanics calculations have been performed. The relative stabilities calculated for each kind of molecule (semi-fluorinated (F) or non-fluorinated (H)) in terms of i) the adsorption of molecules on graphite and ii) the interaction between the molecules have been compared. In a first step, we have calculated the adsorption energy of the single molecules on graphite. In a next step, in order to obtain information on the intermolecular interactions, the energy of several sets of three molecules adsorbed on graphite has been determined. We have considered four possibilities: Two situations in which a set contains three identical molecules (HHH or FFF) and two cases in which a set contains both types of molecules (HFH or FHF). Such a set reflects the orientation of three adjacent molecules in a lamella, the alkyl chains are interdigitated and the distance between the isophthalic acid groups is in the 9.585–9.900 Å range, and allows for quantification of the intermolecular interactions within a lamella. Note that this approach does not take the hydrogen-bonding interactions between ISA groups in adjacent lamellae into account. We assume that these hydrogen bonds do not differ between semi-fluorinated or non-fluorinated molecules, and as such do not contribute to the difference in intermolecular interactions reported below.

The total energies calculated for the systems with one $F_{12}H_6$-ISA (F) or H_{18}-ISA (H) molecule physisorbed on graphite, hereafter noted as $E_{\mathrm{F/graphite}}$ and $E_{\mathrm{H/graphite}}$, are -2.1 and $-36.7\ \mathrm{kcal\,mol^{-1}}$, respectively. Thus, the interaction between the non-fluorinated molecule and graphite is clearly more favorable ($\Delta E = 34.6\ \mathrm{kcal\,mol^{-1}}$), than that between the semi-fluorinated compound and graphite. The difference in stability can be explained on the basis of previous quantum-chemical results (obtained at the ab initio level) which show that besides induced dipole-induced dipole interactions (present in all complexes) another phenomenon playing a significant role in the stability of the alkyl chain/graphite complex is the formation of weak "hydrogen-bond-like" interactions between the $-CH_2$ units and the π-system of graphite.[18b] Moreover, the C–H bond is slightly polarized as the hydrogen atom points towards graphite, which is electron rich. Obviously, no such interaction is established between the $-CF_2$ units and graphite. Furthermore, the $-CF_2$ units are located slightly further from the carbon plane than the $-CH_2$ units (on the order of 0.4 Å for the C atoms and 0.2 Å for the F atoms). In fact, the mean distance between the H and F atoms and the graphite plane is on the order of 2.846 and 3.041 Å, respectively. This also points to a weaker interaction of the $-CF_2$ units with the surface.

The total energies corresponding to three H molecules ($E_{\mathrm{HHH/graphite}}$) or three F molecules ($E_{\mathrm{FFF/graphite}}$) assembled on the carbon plane are on the order of -150.4 and $-42.8\ \mathrm{kcal\,mol^{-1}}$, respectively. We obtain, by combining these results, that the intermolecular interaction energies between three interdigitated H_{18}-ISA molecules (E_{HHH}) and between three interdigitated $F_{12}H_6$-ISA molecules (E_{FFF}) are -40.2 and $-36.4\ \mathrm{kcal\,mol^{-1}}$, respectively. Note that these two values are nearly the same, which is not surprising since the structure of the molecules is quite similar.

Finally, two cases of mixed lamellae of semi-fluorinated and non-fluorinated compounds deposited on graphite have been considered: one where a semi-fluorinated molecule is surrounded by two non-fluorinated chains (HFH), the second one corresponding to the reverse situation (FHF). The total energies of these two systems ($E_{\mathrm{HFH/graphite}}$ and $E_{\mathrm{FHF/graphite}}$) are $-109.3\ \mathrm{kcal\,mol^{-1}}$ and $-77.2\ \mathrm{kcal\,mol^{-1}}$, respectively. The intermolecular interaction energy between one semi-fluorinated molecule and two non-fluorinated molecules surrounding the semi-fluorinated one (E_{HFH}) can be estimated with the following Equation:

$$E_{\mathrm{HHH/graphite}} = E_{\mathrm{HFH/graphite}} - E_{\mathrm{F/graphite}} + E_{\mathrm{H/graphite}} - E_{\mathrm{HFH}} + E_{\mathrm{HHH}} \quad (1)$$

In this way, we have calculated that E_{HFH} is about $-33.8\ \mathrm{kcal\,mol^{-1}}$, that is $6.4\ \mathrm{kcal\,mol^{-1}}$ lower than the interaction energy between three non-fluorinated molecules (E_{HHH}). This difference in intermolecular interaction energy, in combination with the relatively unfavorable adsorption energy of a single semi-fluorinated molecule on graphite, accounts for the gradual replacement of semi-fluorinated molecules by non-fluorinated molecules.[20] It should be clear that a desorption–readsorption process also holds for non-fluorinated molecules, which goes unnoticed except in those rare cases where such a molecule is replaced by a semi-fluorinated one. Based upon the previous calculations, one might expect a longer residence time for the non-fluorinated molecules.

One has to keep in mind that the influence of the solvent on the energetics of adsorption and the entropic contributions have been neglected in the present calculations.

Although the desorption sometimes occurs while the tip is scanning over the molecule (Figure 5d), in general we find that desorption takes place in between succesive scans (Figure 5e–f). Furthermore, on some occasions we could observe that within one lamella a semi-fluorinated molecule desorbs while a second one remains adsorbed. In combination with the relatively long residence times, this suggests an only minor influence of the STM tip on the observed molecular dynamics.

All STM experiments described in this paper are performed in solution. Hence, there is an equilibrium between the molecules adsorbed on the graphite surface and those in the supernatant solution. A mathematical model for such two-component system has been devised by Venkataraman et al.[7] The resulting equation that describes this system is reminiscent of the Langmuir model for the gas/solid interface. This equation was further adapted by Venkataraman et al. with the assumption that there is no interaction between the solute and the solvent molecules. Hence, this model is not suitable to evaluate our experimental findings, since the isophthalic acid head groups can form hydrogen bonds with the hydroxyl group of an alcohol molecule. Furthermore, in case of the mixtures of fluorinated and non-fluorinated isopthalic acid derivatives a three-component system has to be considered. In addition, the fluorinated and non-fluorinated isopthalic acid derivatives are interacting species since they do not assemble on the graphite surface in separate domains.

Conclusion

Dynamics occurring in monolayers of isophthalic acid derivatives at the liquid/solid interface have been investigated with a commercial STM and with a home-built video-STM in real-time (two frames per second). When using octan-1-ol or undecan-1-ol as solvents for the 5-alkoxy-isophthalic acid derivatives, these solvent molecules co-adsorb in the monolayer structure. In this manner a two-dimensional co-crystal is formed. This solvent co-deposition has for the first time been visualized in real-time (two frames per second). From a quantitative analysis we find residence times of at least 15 ms for the physisorbed molecules. The overall structure of the monolayer was found to be stable for at least 0.5 s, while the exchange rate of solvent molecules was determined to be faster than 0.5 s. For these systems it was not possible to determine an actual residence time of individual molecules. This difficulty has been overcome by use of labeled molecules, namely semi-fluorinated molecules.

For mixtures of semi-fluorinated and non-fluorinated isophthalic acid derivatives dynamic phenomena in seemingly static monolayers which would otherwise go unnoticed could be detected as well. The observations could be made easily since the fluorocarbon segments serve as a probe for the interpretation of the obtained images. While imaging the same region of a monolayer for an extended period of time we observed that non-fluorinated molecules progressively substitute the fluorinated molecules. From molecular mechanics calculations we propose that this phenomenon can primarily be attributed to the substantially smaller adsorption energy of a semi-fluorinated molecule physisorbed on graphite compared with a non-fluorinated molecule. In addition, there is also a small difference in intermolecular interaction energy. Furthermore, the perfluorinated part of the alkyl chain of a semi-fluorinated molecule is located slightly further from the graphite plane than the hydrogenated part of the alkyl chain. The residence time of the semi-fluorinated molecules ranges from a few seconds to several minutes. These relatively long times illustrate the stabilizing interactions between the molecules in the monolayer, which are to a large extent based upon hydrogen bonding. However, the exchange process itself is fast and takes less than 4.3 ms.

The co-deposition processes were initiated in the vicinity of domain boundaries, while the exchange of semi-fluorinated molecules by non-fluorinated molecules also took place in densely packed regions. The observed molecular motions and rearrangements in the monolayers are attributed to the process of adsorption and desorption of molecules on the graphite substrate and to rotation and translation of molecules on the surface.

Acknowledgement

The authors thank the DWTC, through IUAP-IV-11, and ESF SMARTON for financial support. A.G. thanks the IWT for a predoctoral scholarship. S.D.F. is a postdoctoral fellow of the Fund for Scientific Research-Flanders. R.L. is Maître de Recherches du Fonds National de la Recherche Scientifique. The collaboration was made possible thanks to the TMR project SISITOMAS and IUAP.

[1] a) J. P. Rabe, S. Buchholz, *Science* **1991**, *253*, 424 – 427; b) D. M. Cyr, B. Venkataraman, G. W. Flynn, *Chem. Mater.* **1996**, *8*, 1600 – 1615; c) G. C. McGonical, R. H. Bernhardt, D. J. Thomson, *Appl. Phys. Lett.* **1990**, *57*, 28 – 30.

[2] a) F. Stevens, D. J. Dyer, D. M. Walba, *Angew. Chem.* **1996**, *108*, 955 – 957; *Angew. Chem. Int. Ed. Engl.* **1996**, *35*, 900 – 901; b) D. M. Walba, F. Stevens, N. A. Clark, D. C. Parks, *Acc. Chem. Res.* **1996**, *29*, 591 – 597; c) S. De Feyter, P. C. M. Grim, M. Rücker, P. Vanoppen, C. Meiners, M. Sieffert, S. Valiyaveettil, K. Müllen, F. C. De Schryver, *Angew. Chem.* **1998**, *110*, 1281 – 1284; *Angew. Chem. Int. Ed.* **1998**, *37*, 1223 – 1226; d) S. De Feyter, A. Gesquière, P. C. M. Grim, S. Valiyaveettil, C. Meiners, M. Sieffert, K. Müllen, F. C. De Schryver, *Langmuir* **1999**, *15*, 2817 – 2822.

[3] a) R. Heinz, A. Stabel, J. P. Rabe, G. Wegner, F. C. De Schryver, D. Corens, W. Dehaen, C. Süling, *Angew. Chem.* **1994**, *106*, 2154 – 2157; *Angew. Chem. Int. Ed. Engl.* **1994**, *33*, 2080 – 2083; A. Stabel, P. Herwig, K. Müllen, J. P. Rabe, *Angew. Chem.* **1995**, *107*, 1768 – 1770; *Angew. Chem. Int. Ed. Engl.* **1995**, *34*, 1609 – 1611; b) P. C. M. Grim, P. Vanoppen, M. Rücker, S. De Feyter, S. Valiyaveettil, G. Moessner, K. Müllen, F. C. De Schryver, *J. Vac. Sci. Technol. B* **1997**, *15*, 1419 – 1424; c) P. C. M. Grim, S. De Feyter, A. Gesquière, P. Vanoppen, M. Rücker, S. Valiyaveettil, G. Moessner, K. Müllen, F. C. De Schryver, *Angew. Chem.* **1997**, *109*, 2713 – 2715; *Angew. Chem. Int. Ed. Engl.* **1997**, *36*, 2601 – 2603.

[4] A. Stabel, R. Heinz, J. P. Rabe, G. Wegner, F. C. De Schryver, *J. Phys. Chem.* **1995**, *99*, 8690 – 8697.

[5] A. Stabel, R. Heinz, F. C. De Schryver, J. P. Rabe, *J. Phys. Chem.* **1995**, *99*, 505 – 507.

[6] L. Askadskaya, J. P. Rabe, *Phys. Rev. Lett.* **1992**, *69*, 1395 – 1398.

[7] B. Venkataraman, J. J. Breen, G. W. Flynn, *J. Phys. Chem.* **1995**, *99*, 6608 – 6619.

[8] N. Elbel, W. Roth, E. Günther, H. von Seggern, *Surf. Sci.* **1994**, *303*, 424 – 432.

[9] M. Hibino, A. Sumi, I. Hatta, *Thin Solid Films* **1996**, *273*, 272 – 278.

[10] S. Valiyaveettil, C. Gans, M. Klapper, R. Gereke, K. Müllen, *Polym. Bull.* **1994**, *34*, 13.

[11] a) M. S. Vollmer, F. Effenberger, R. Stecher, B. Gompf, W. Eisenmenger, *Chem. Eur. J.* **1999**, *5*, 96 – 101; b) J. Wintterlin, J. Trost, S. Renisch, R. Schuster, T. Zambelli, G. Ertl, *Surf. Sci.* **1997**, *394*, 159 – 169; c) M. Eer, K. Morgenstern, G. Rosenfeld, G. Comsa, *Surf. Sci.* **1998**, *402 – 404*, 341 – 345; d) C. Ludwig, B.Gompf, W. Glatz, J. Petersen, W. Eisenmenger, M. Möbus, U. Zimmermann, N. Karl, *Z. Phys. B* **1992**, *86*, 397 – 404.

[12] A. K. Rappé, C. J. Casewit, K. S. Colwell, W. A. Goddard III, and W. M. Skiff, *J. Am. Chem. Soc.* **1992**, *114*, 10024 – 10035.

[13] C. J. Casewit, K. S. Colwell, A. K. Rappé, *J. Am. Chem. Soc.* **1992**, *114*, 10035 – 10046.

[14] R. Lazzaroni, A. Calderone, G. Lambin, J. P. Rabe, J. Brédas, *Synth. Met.* **1991**, *525*, 41 – 43.

[15] P. Vanoppen, P. C. M. Grim, M. Rücker, S. De Feyter, G. Moessner, S. Valiyaveettil, K. Müllen, F. C. De Schryver, *J. Phys. Chem.* **1996**, *100*, 19636 – 19641.

[16] A. Gesquière, M. M. Abdel-Mottaleb, M. Sieffert, K. Müllen, F. C. De Schryver, *Langmuir* **1999**, *15*, 6821 – 6824.

[17] A. Stabel, L. Dasaradhi, D. O'Hagan, J. P. Rabe, *Langmuir* **1995**, *11*, 1427 – 1430.

[18] a) G. Lambin, A. Calderone, R. Lazzaroni, J. L. Brédas, T. C. Clarke, J. P. Rabe, *Mol. Cryst. Liq. Cryst.* **1993**, *235*, 75; b) R. Lazzaroni, A. Calderone, J. L. Brédas, J. P. Rabe, *J. Chem. Phys.* **1997**, *107*, 99 – 105.

[19] F. Stevens, T. P. Beebe, Jr., *Langmuir* **1999**, *15*, 6884 – 6889.

[20] This difference in stabilization energy also accounts for the low ratio of semi-fluorinated molecules with respect to non-fluorinated molecules in the observed mixed monolayers, even though the solution from which the monolayer is formed has a 1:1 molar ratio. Similarly, it accounts for the preferential readsorption of non-fluorinated molecules.

Received: September 22, 1999
Revised version: February 11, 2000 [F2050]

 © WILEY-VCH Verlag GmbH, D-69451 Weinheim, 2000 0947-6539/00/0620-3746 $ 17.50+.50/0